



Recent results on ECAL-P developments for the LUXE experiment

Aleksander Filip Żarnecki
University of Warsaw

ILD monthly meeting
May 12, 2026

1 Motivation

- Non-linear QED
- Strong field QED

2 LUXE experiment

- Concept
- Operation modes
- Physics highlights

LUXE

ECAL-P group:



UNIVERSITY
OF WARSAW



TEL AVIV UNIVERSITY



members of DRDCalo and new FCAL collaborations

3 ECAL-P for LUXE

- Design concept
- 2025 prototype

4 Beam test results

- Event reconstruction
- Energy resolution and shower profile
- Beam telescope alignment
- Measurements with beam telescope

5 Conclusions

LUXE

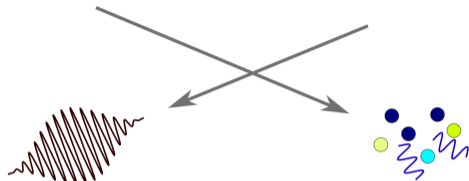
ECAL-P group:



members of DRDCalo and new FCAL collaborations

Classical nonlinearity

In most beam-beam collisions we can assume that only two particles interact, one from each beam. This can be very different in beam-laser interactions...

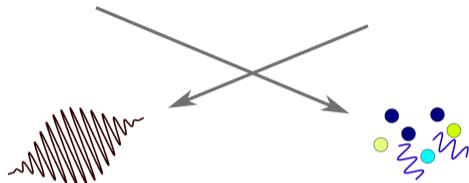


B.King @ LUXE Coll. 2023

Laser pulse is a coherent state: multi-photon interactions possible...

Classical nonlinearity

In most beam-beam collisions we can assume that only two particles interact, one from each beam. This can be very different in beam-laser interactions...



B.King @ LUXE Coll. 2023

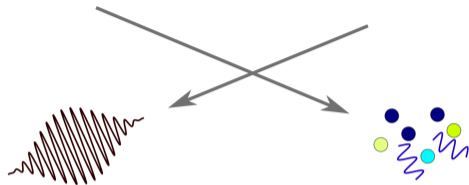
Laser pulse is a coherent state: multi-photon interactions possible...

We can try to estimate the expected number of photons participating in the single collision:

- the characteristic scale of the interaction is the **Compton wavelength**: $\lambda_C = \frac{\hbar}{mc}$
- **work** of the **laser electric field** \mathcal{E}_L can be estimated as $\Delta E = e\mathcal{E}_L \cdot \lambda_C$
- **number of laser photons** contributing to this energy transfer: $\xi = \frac{\Delta E}{\hbar\omega_L}$

Classical nonlinearity

In most beam-beam collisions we can assume that only two particles interact, one from each beam. This can be very different in beam-laser interactions...



B.King @ LUXE Coll. 2023

Laser pulse is a coherent state: multi-photon interactions possible...

We can try to estimate the expected number of photons participating in the single collision:

- the characteristic scale of the interaction is the **Compton wavelength**: $\lambda_C = \frac{\hbar}{mc}$
- **work** of the **laser electric field** \mathcal{E}_L can be estimated as $\Delta E = e\mathcal{E}_L \cdot \lambda_C$
- **number of laser photons** contributing to this energy transfer: $\xi = \frac{\Delta E}{\hbar\omega_L}$

The resulting number is called the **classical nonlinearity parameter**

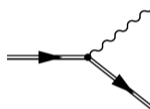
$$\xi = \frac{e\mathcal{E}_L \cdot \lambda_C}{\hbar\omega_L} = \frac{e\mathcal{E}_L \cdot \lambda_L}{mc^2}$$

Processes of interest

double line denotes Volkov state - electron interacting with the “background” laser field

- Non-linear Compton scattering

$$e^- + n\omega_L \rightarrow e^- + \gamma$$

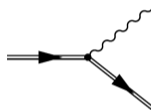


Processes of interest

double line denotes Volkov state - electron interacting with the “background” laser field

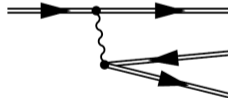
- Non-linear Compton scattering

$$e^- + n\omega_L \rightarrow e^- + \gamma$$



- Non-linear trident process

$$e^- + n\omega_L \rightarrow e^- + e^+ e^-$$

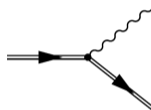


Processes of interest

double line denotes Volkov state - electron interacting with the “background” laser field

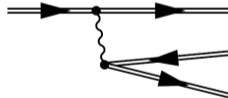
- Non-linear Compton scattering

$$e^- + n\omega_L \rightarrow e^- + \gamma$$



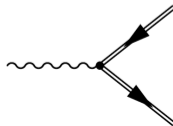
- Non-linear trident process

$$e^- + n\omega_L \rightarrow e^- + e^+ e^-$$



- Non-linear Breit-Wheeler process

$$\gamma + n\omega_L \rightarrow e^+ + e^-$$



Quantum nonlinearity

For extremely high electric field, work over the Compton wavelength can exceed electron mass.

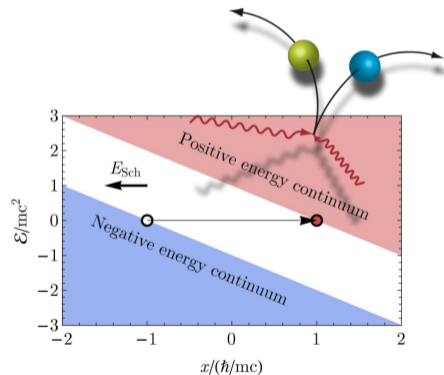
Critical field, also known as the Schwinger limit:

J. Schwinger, Phys. Rev. 82, 664 (1951)

$$e \mathcal{E}_{cr} \cdot \lambda_C = m c^2$$

$$\mathcal{E}_{cr} \approx 1.3 \cdot 10^{18} \text{ V/m}$$

For fields comparable or higher than the critical field, e^+e^- pairs can be created by tunneling from vacuum.



T. Blackburn @ LUXE Coll. 2024

Quantum nonlinearity

For extremely high electric field, work over the Compton wavelength can exceed electron mass.

Critical field, also known as the **Schwinger limit**:

J. Schwinger, Phys. Rev. 82, 664 (1951)

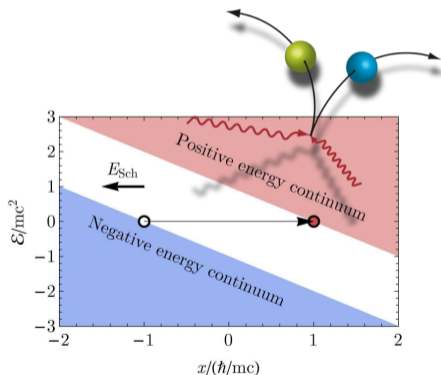
$$e \mathcal{E}_{cr} \cdot \lambda_C = m c^2$$

$$\mathcal{E}_{cr} \approx 1.3 \cdot 10^{18} \text{ V/m}$$

For fields comparable or higher than the critical field, e^+e^- pairs can be created by tunneling from vacuum.

Quantum nonlinearity parameter:

$$\chi = \frac{\mathcal{E}}{\mathcal{E}_{cr}} = \frac{\hbar \omega_L}{m c^2} \xi$$



T. Blackburn @ LUXE Coll. 2024

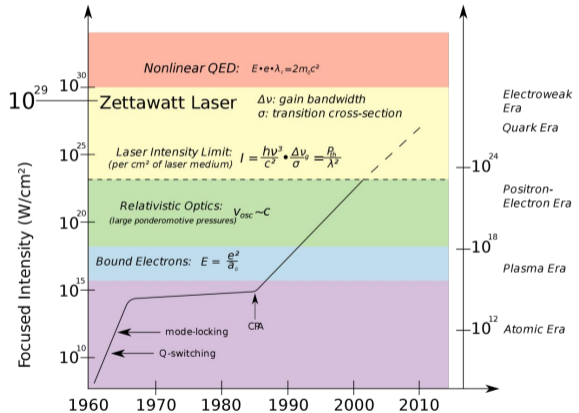
Experimental reach

Rapid progress in high-intensity lasers.

With Chirped Pulse Amplification (CPA) we can reach TW – PW power, electric fields up to

$$\mathcal{E} \sim 10^{14} \text{ V/m}$$

Still orders of magnitude below \mathcal{E}_{cr} ...



T. Blackburn @ LUXE Coll. 2024

Experimental reach

Rapid progress in high-intensity lasers.

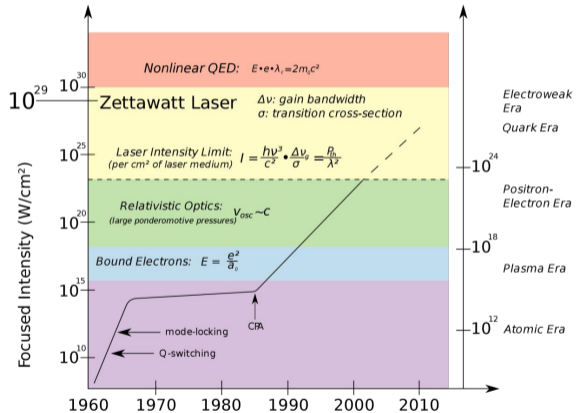
With Chirped Pulse Amplification (CPA) we can reach TW – PW power, electric fields up to

$$\mathcal{E} \sim 10^{14} \text{ V/m}$$

Still orders of magnitude below $\mathcal{E}_{cr} \dots$

But the field can be much higher for the relativistic electron colliding head-on with the laser pulse:

$$\mathcal{E}^* = \gamma \mathcal{E}_{LAB} (1 + \cos \theta)$$



T. Blackburn @ LUXE Coll. 2024

LUXE

Laser Und XFEL Experiment

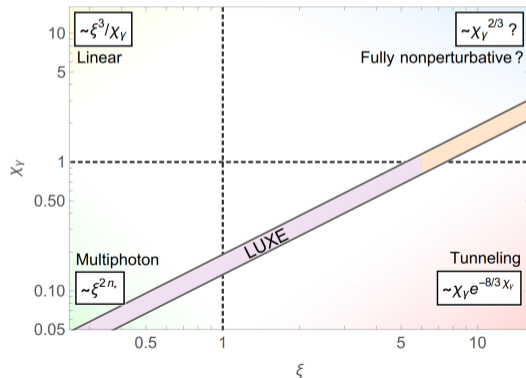
Probing SF QED in collisions of ultra-relativistic EuXFEL beam with high-power laser pulses

Designed to make precision measurements of the transition from perturbative to non-perturbative QED regime and test theoretical predictions in the previously unexplored domain

$$\xi \lesssim \mathcal{O}(10)$$

$$\chi \lesssim \mathcal{O}(1)$$

in both electron-laser and photon-laser collisions.

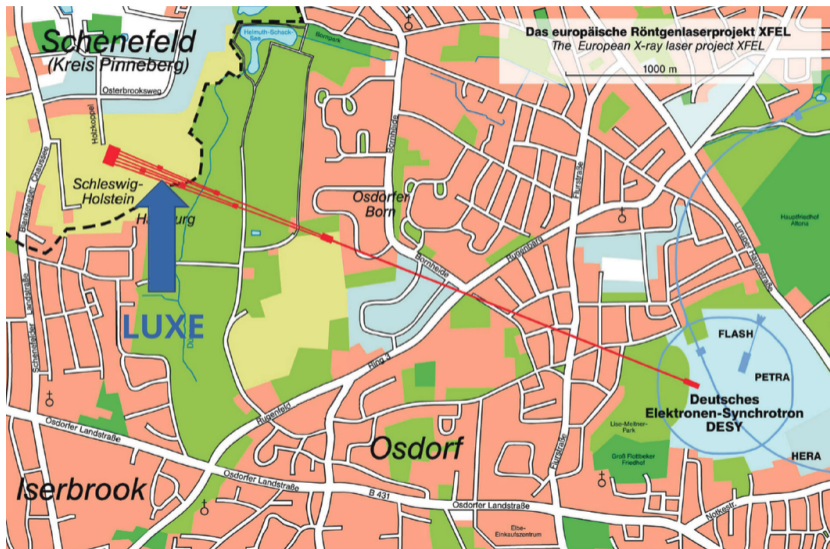


Concept

EuXFEL electron beam:

- 16.5 GeV
 - 10 Hz bunch trains
 - $1.5 \cdot 10^9 e^-$ /bunch
- 1 out of 2700 for LUXE

New extraction beamline funded through ELBEX grant (Horizon Europe)



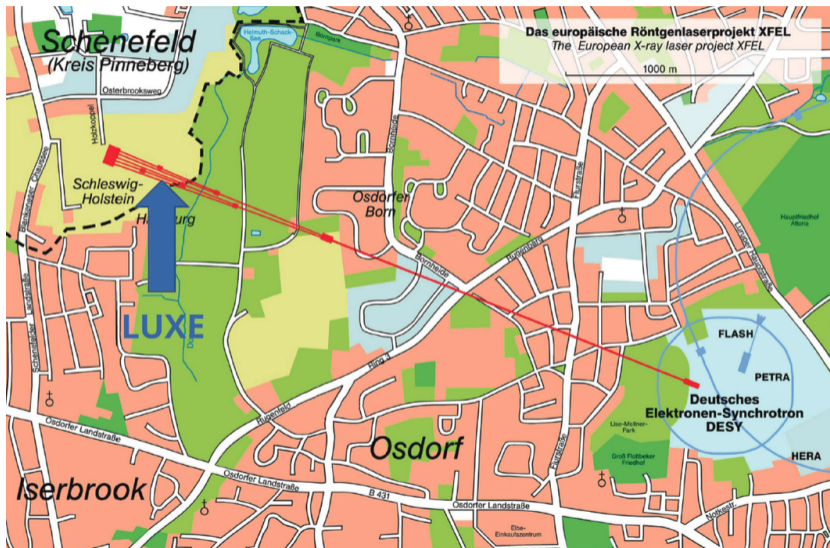
Concept

Laser system

- Ti:Sa laser 800 nm
- 40 TW in “phase-0”
350 TW in “phase-1”
- 30 fs pulses at 1 Hz
- 3 μm beam spot

10 TW optical laser
JeTi40 already at DESY
loan from FSU Jena

⇒ could start in 2030...



Operation modes

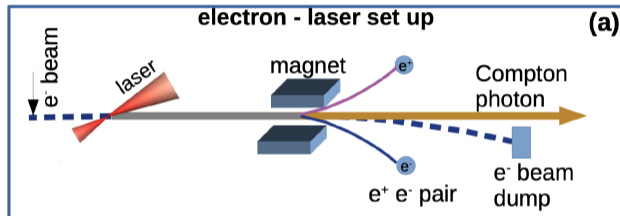
- **electron-laser**

Up to 10^9 photons and electrons per pulse

⇒ dedicated instruments needed for precise spectra and flux measurement.

$10^{-3} - 10^5$ positrons per pulse

⇒ “standard” high precision tracking and **highly compact calorimeter**



Operation modes

● electron-laser

Up to 10^9 photons and electrons per pulse

⇒ dedicated instruments needed for precise spectra and flux measurement.

$10^{-3} - 10^5$ positrons per pulse

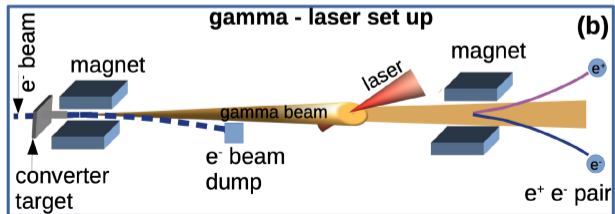
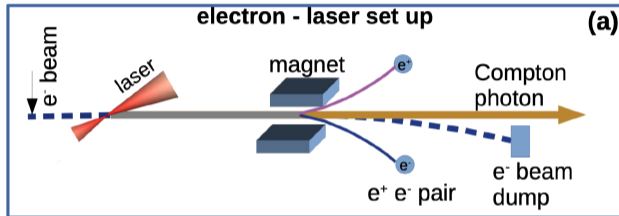
⇒ “standard” high precision tracking and highly compact calorimeter

● gamma-laser

Up to 10^9 photons per pulse

and $10^{-5} - 10$ $e^+ e^-$ pairs

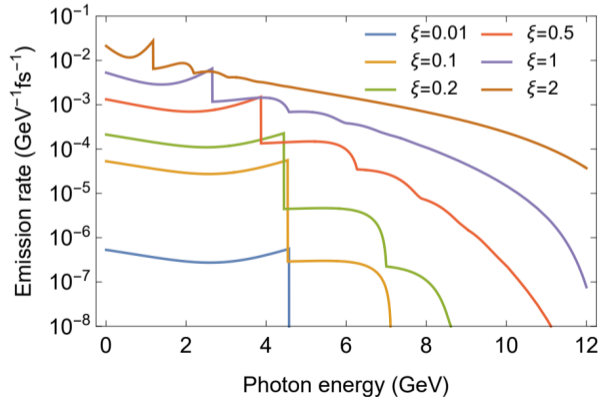
⇒ high precision tracking and calorimetry also for electron spectra measurement



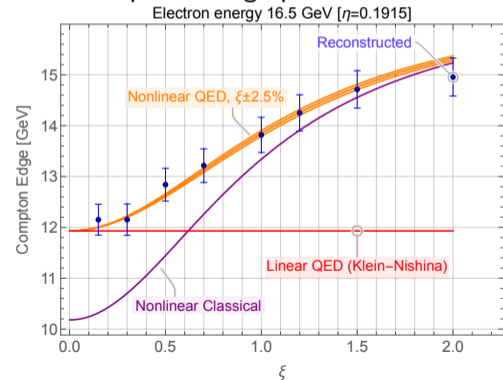
Compton edge electron-laser mode

Expected changes in the observed Compton spectra as a function of ξ parameter:

Photon spectra shape



Electron spectra edge position

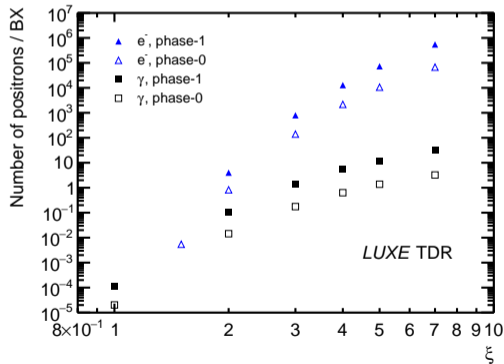


arXiv:2308.00515

e^+e^- pair production

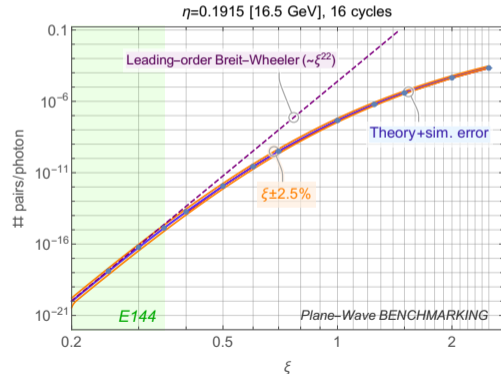
Expected positron production rate as a function of ξ parameter:

Flux for different running scenarios



electron-laser and gamma-laser interactions

Theory and measurement precision



gamma-laser interactions

Design concept

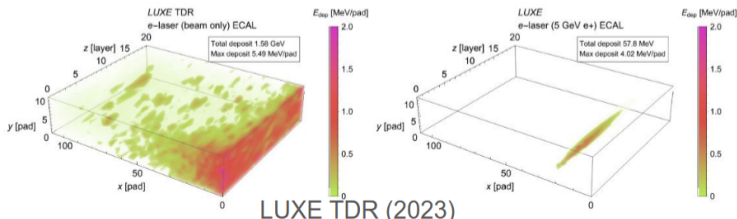
Main challenge for positron detection:

expected number of positrons varying from 10^{-4} to 10^7 per laser pulse (!)

Two running modes planned for positron calorimeter, for low and high intensity:

- at low intensity showers need to be identified in a widely spread background
- at high intensity shower will overlap \Rightarrow only total flux reconstruction possible

For both modes, precision depends on the transverse shower size !



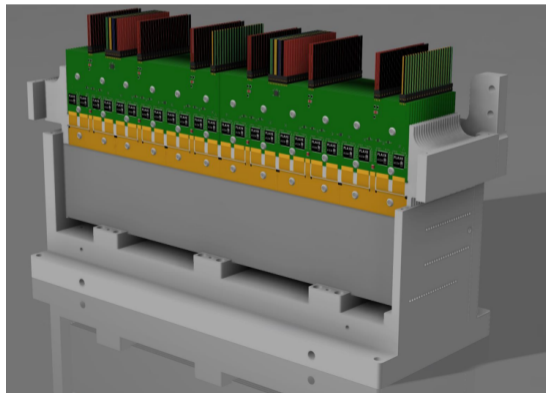
Design concept

Highly compact and modular calorimeter to minimize the Molière radius. Design based on the concept of **forward calorimeters** developed for luminosity measurement at future e^+e^- colliders. Based on thin silicon sensors previously produced for CALICE (16×16 pads 5.5×5.5 mm²).

- 21 tungsten plates of $1 X_0$
- 1 mm sensor gaps between
- 20 active planes
- six sensors per plane
- Front-End-Boards (FEB) above the sensors

Requires dedicated sensor sandwich design, dedicated FEB, readout scheme and mechanics.

Design developed for LUXE TDR (2023) \Rightarrow

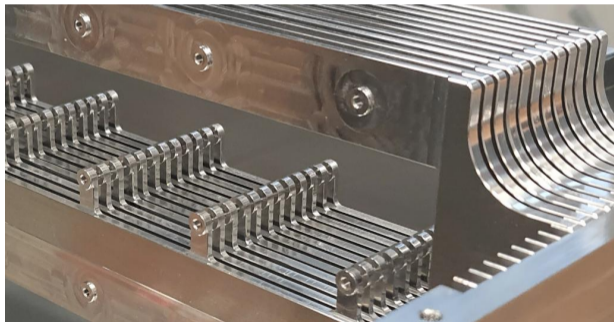
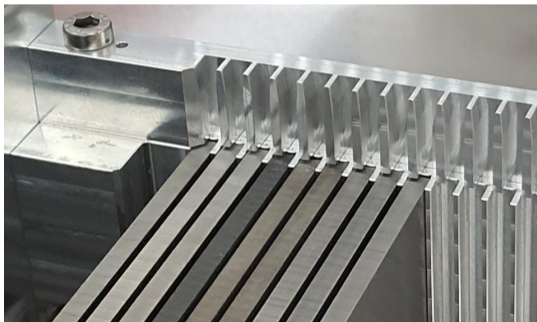


Mechanical frame

Aluminum frame designed and manufactured at University of Warsaw (machined to $10\ \mu\text{m}$)

Tungsten plates from three vendors:

“T-frames” for FEB and sensor support:



Nominal sensor gap increased to 1.2 mm to secure min. of 1.0 mm clearance...

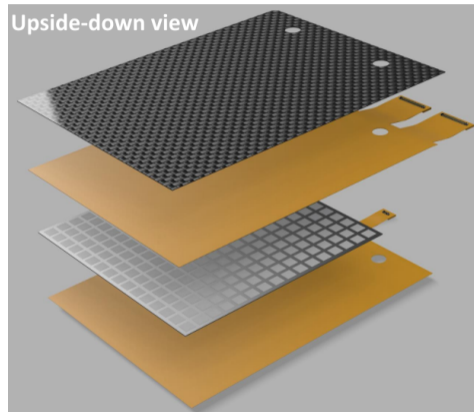
Compact Silicon Sandwich - CSIS

Prototype sensor structure:



Includes HV Kapton, silicon sensor, signal Kapton, carbon fiber support to improve mechanical properties

Total thickness (including glue): 800 – 850 μm .



20 CSIS produced at IFIC Valencia

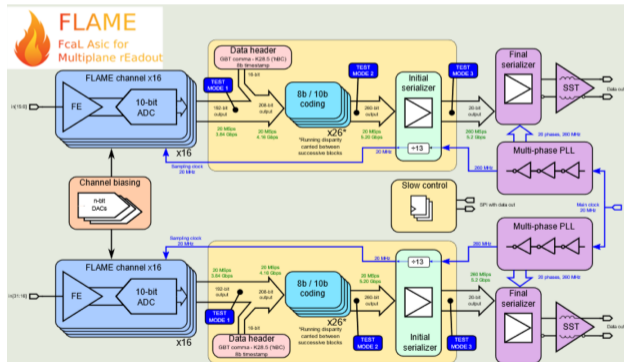
Front-end electronics

Based on FCAL FLAME ASIC,
previously developed for the luminosity detector at future Higgs factory

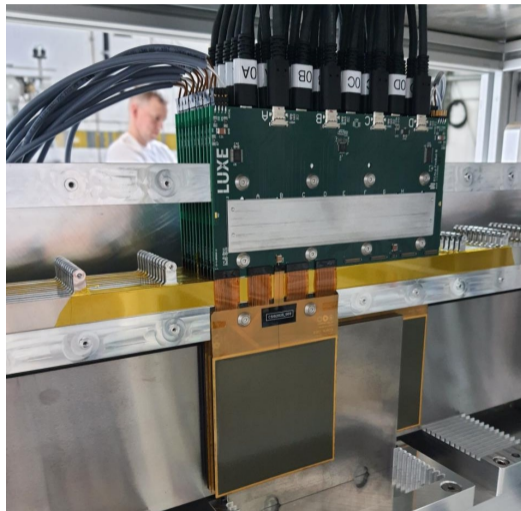
Main features:

- 32 channels
- 10 bit ADC at 20 MHz in each channel
- Analog front-end in each channel.
CR-RC shaper of 50 ns
- High speed serializer

Read out with dedicated system based on
commercial Trenz TE0808 FPGA
Developed at AGH Krakow



Prototype at DESY test beam, June 2025

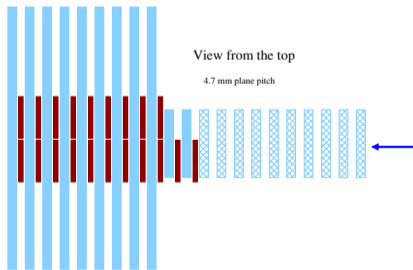


Test setup

20 sensors in 11 planes

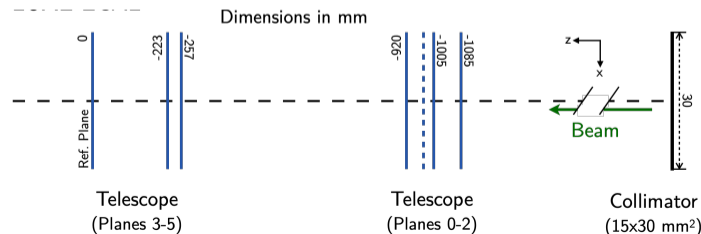
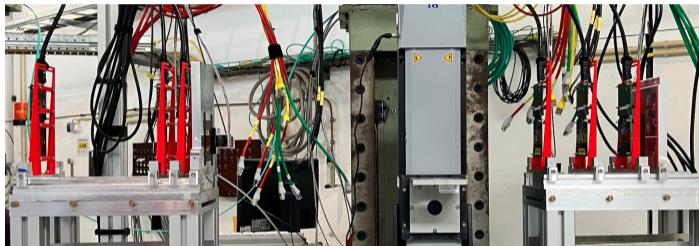
Two running configurations:

- without absorber (tracker mode)
- with 11 to 21 tungsten plates (calorimeter mode)



New ALPIDE telescope

electron position to $\sim 40 \mu\text{m}$

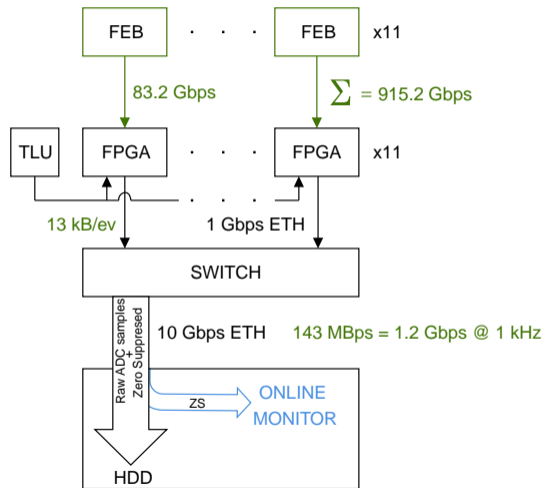


DAQ

Two streams of data were stored:

- Zero Suppressed (ZS) data calculated signal amplitude and arrival time for triggered channels from FPGA **crucial for on-line monitoring**
- Raw ADC samples for all channels **used in off-line event reconstruction and analysis**, crucial for understanding of detector performance

Raw data consumes around 250 times more storage space in comparison to ZS data.



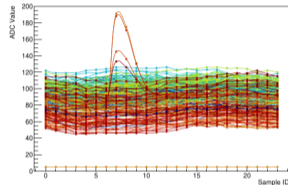
Worked without problems up to 2 kHz event rate, over 300 million events collected (33 TB) !!!

Signal processing

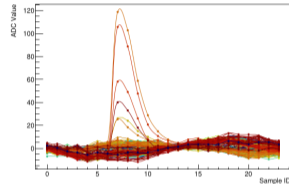
Processing of sampled signals:

- bad channels are eliminated,
- pedestal subtraction is applied, signal candidates are identified,
- common mode is subtracted, as calculated from non-signal channels,
- signal candidate selection is repeated, additional filter and correction is applied,
- integral non-linearity correction is applied for large signals

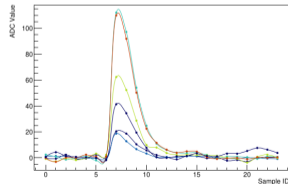
1. ADC samples



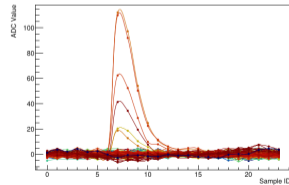
2. Pedestal subtracted



3. Signal candidates



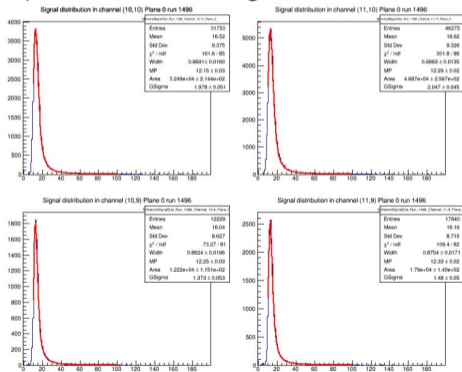
4. Pedestal and CM subtracted



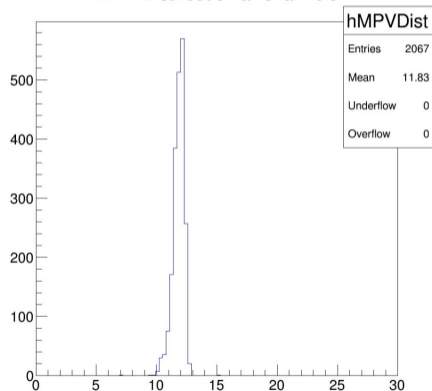
Channel calibration

Based on data collected without absorber planes (tracker mode) - “MIP” signal

Example fit results for single channels:



MPV Distribution all channels

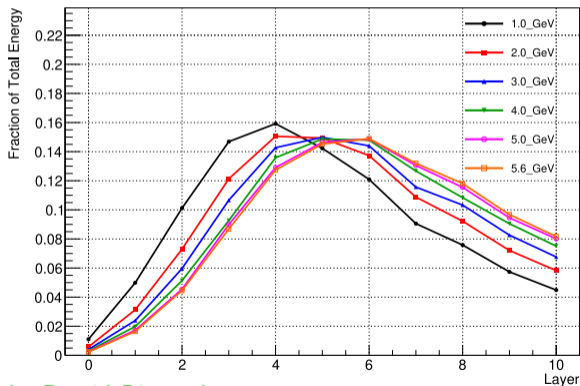


by Melissa Almanza Soto

Longitudinal shower profile

Average signal per layer from calorimeter mode runs with different beam energies.

Deposited Energy vs Layer



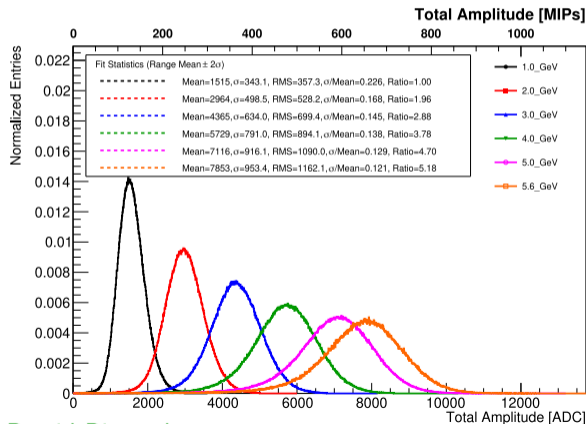
- Shower profile scaling with $\ln(E)$
- Prototype limited to $11 X_0$
- Too shallow for higher electron energies

Dedicated runs with additional tungsten plates in front of the prototype still to be included in the analysis

by Dawid Pietruch

Energy resolution

Signal distribution and resolution from calorimeter mode runs with different beam energies.

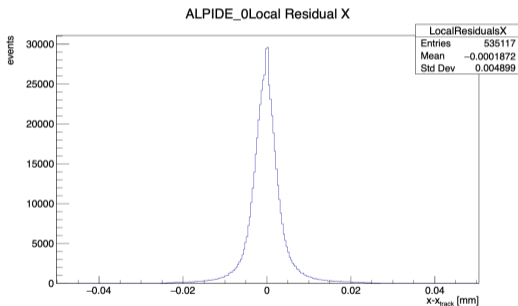
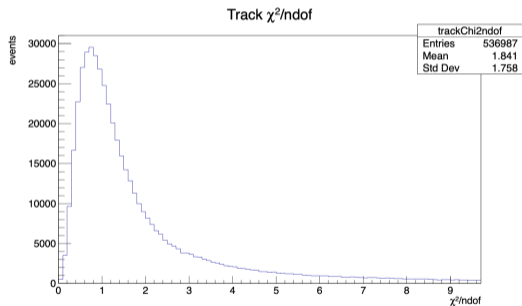


- Expected response distribution at low energies
- Visible non-linearity due to longitudinal leakages
- Also affecting distribution shape \Rightarrow energy resolution

by Dawid Pietruch

Telescope track reconstruction

ALPIDE sensors ($29 \times 27 \mu\text{m}^2$ pixels) measure track position with precision down to $3 \mu\text{m}$. Six-plane track fit performed in [Corryvreckan](#) taking multiple scattering into account.



by Shan Huang

At 5 GeV, track position at the calorimeter face is reconstructed with about $40 \mu\text{m}$ precision.

Dominated by multiple scattering in the last sensor plane.

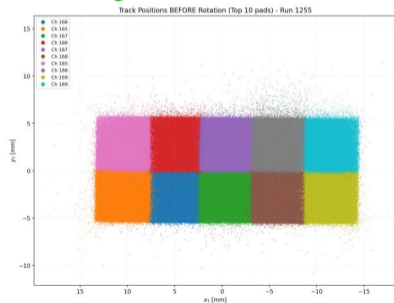
Telescope alignment

Calorimeter and telescope reference frames need to be aligned \Rightarrow two approaches developed

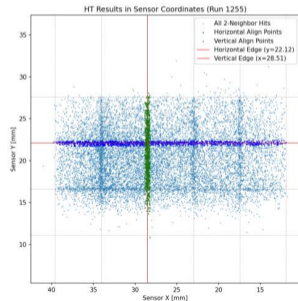
Hough transform method was designed for the tracker mode.

Considered are events with deposits in two neighboring cells - track hitting cell edge

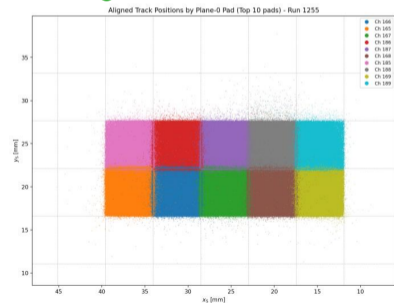
Before alignment



Selected events



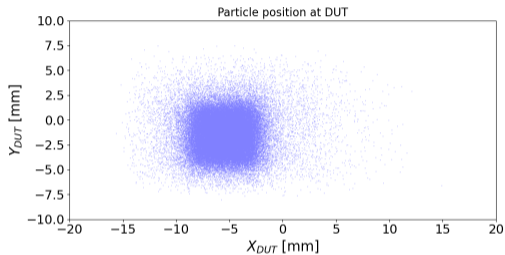
After alignment



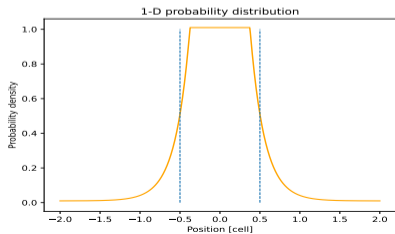
by Michal Elad

Telescope alignment

Likelihood method for calorimeter mode



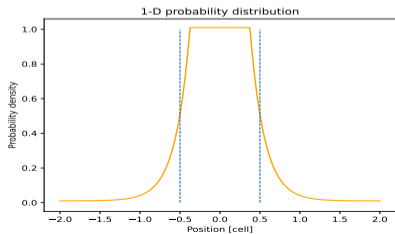
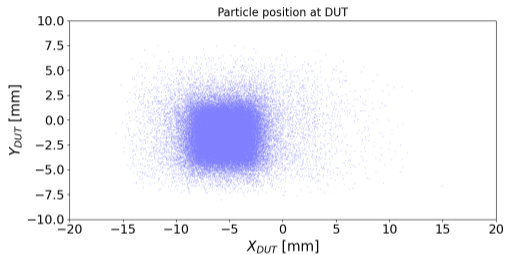
← track position extrapolated from the telescope for the maximum deposit in single cell of layer 9.



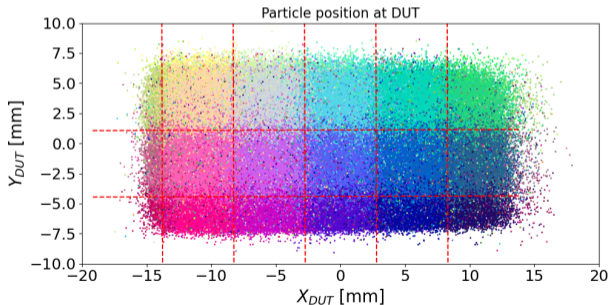
← we can consider probability distribution for finding maximum at given distance from the track.

Telescope alignment

Likelihood method for calorimeter mode



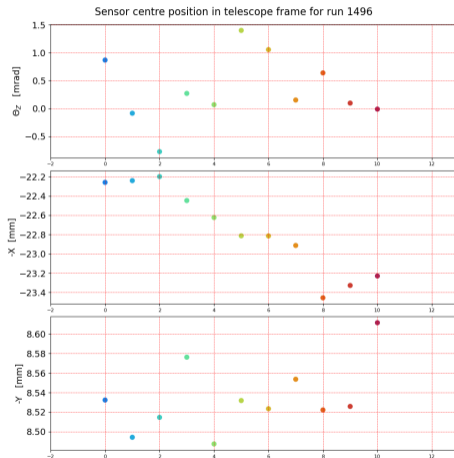
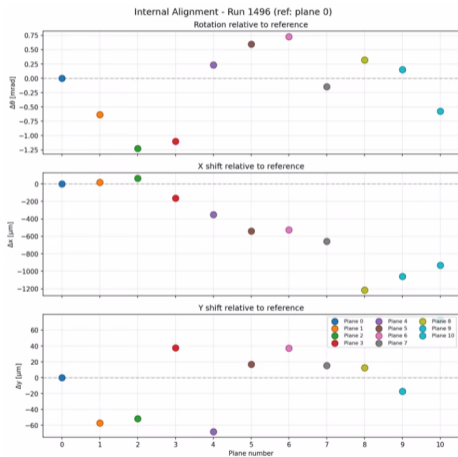
Calorimeter layer can be aligned with the telescope by maximizing the log-likelihood function for large sample of cascade events.



by Bartłomiej Brudnowski

Telescope alignment

Method comparison for tracker mode run



Consistent results from Hough transform (left) and likelihood method (right)

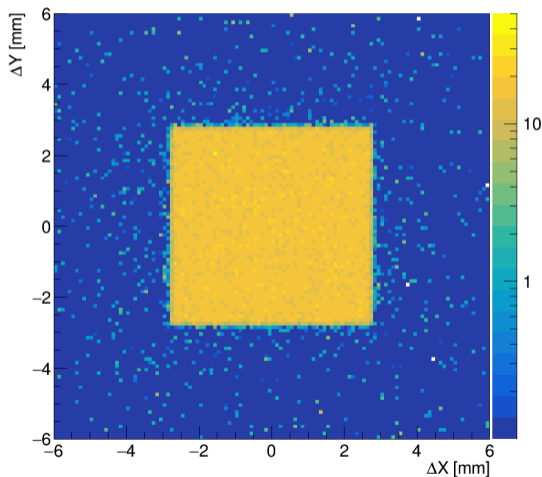
Sensor response studies

Knowing exact position of the track hitting the sensor, we can study sensor response in detail, cell by cell.

We profit from huge statistics of events!

Inner cells: uniform response over $5.53 \times 5.53 \text{ mm}^2$
in perfect agreement with Hamamatsu specification

Response profile for cell 128 in plane 0



Sensor response studies

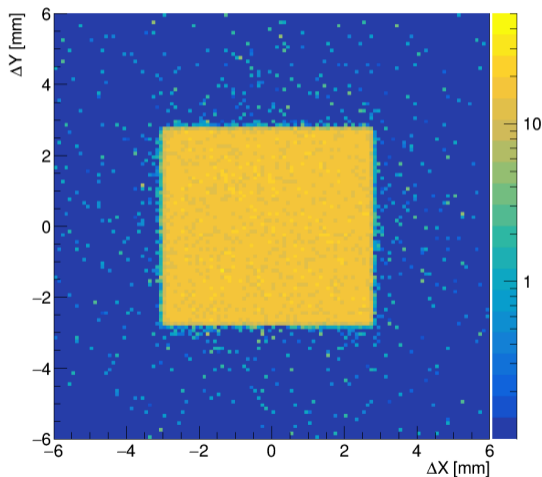
Knowing exact position of the track hitting the sensor, we can study sensor response in detail, cell by cell.

We profit from huge statistics of events!

Inner cells: uniform response over $5.53 \times 5.53 \text{ mm}^2$
in perfect agreement with Hamamatsu specification

Edge cells: significantly larger (by $\sim 0.2 \text{ mm}$).
Total active area slightly larger than specified!

Response profile for cell 131 in plane 0



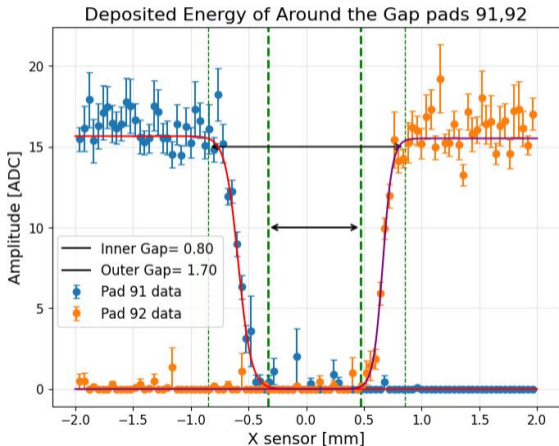
Sensor gap studies - tracker mode

Gap between two sensors (two towers)

- 0.2 mm mechanical clearance
- 2×0.76 mm of uninstrumented silicon
⇒ 1.72 mm of “dead” region expected

With wider edge pixels,
effective gap width significantly reduced!

Only around 1.0 mm with no response at all



by Ben David Talmor

Sensor gap studies - calorimeter mode

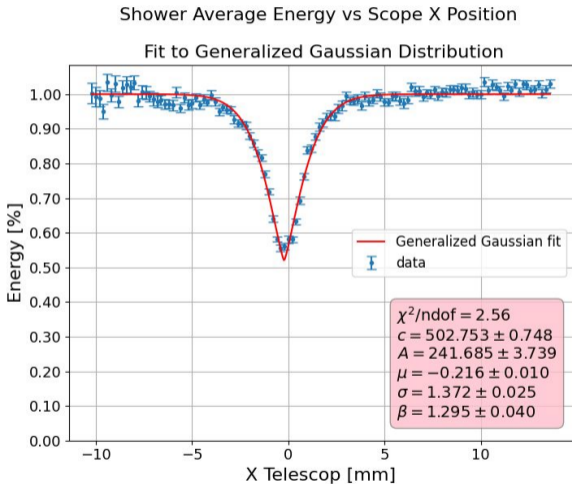
With **very narrow shower core** in tungsten, ~ 1 mm gap can have very strong effect on the calorimeter response.

Response to **perpendicular beam** of 5 GeV electrons as a function of the impact point \Rightarrow

Up 50% signal loss for showers in the gap!

Fortunately, there will be no perpendicular positrons in LUXE (due to magnetic field)

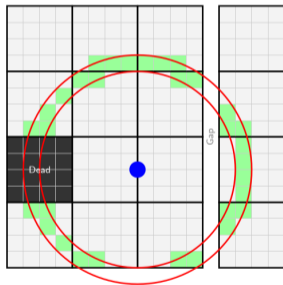
Runs taken with different beam incident angles still to be analyzed



by Ben David Talmor

Molière radius

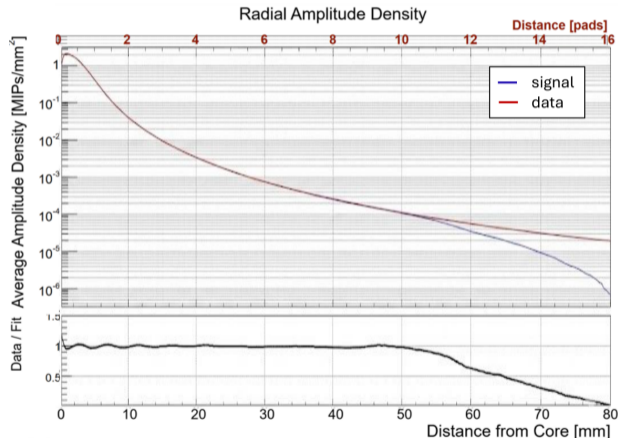
Weighted response calculated in each layer in narrow radial bins:



including correction for non-active cells

Weights calculated from fitted radial profile (iterative procedure)

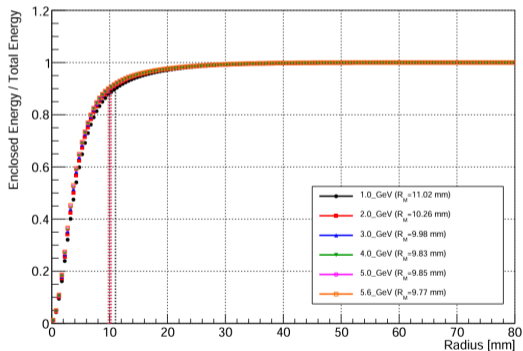
by Dawid Pietruch



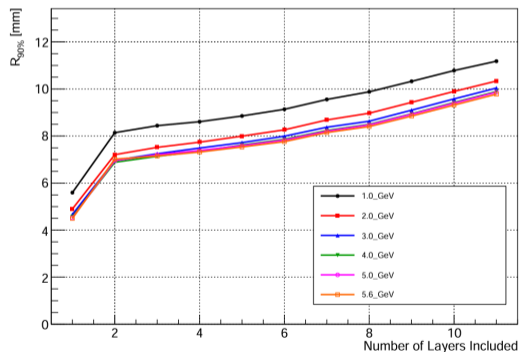
Molière radius

Calculated for increasing number of calorimeter layers (X_0) considered

Cumulative Energy Profile



Moliere Radius Evolution



11 X_0 clearly not sufficient for detailed estimate \Rightarrow runs with addition tungsten in front (WIP)

With LUXE experiment, Strong-Field QED research will enter intensity parameter domain never explored before, but also facing new experimental challenges.

Highly compact positron calorimeter is a key component of the experiment.

Full scale prototype, very close to the final design, built and successfully tested in 2025.

Huge amount of high quality data collected with very precise information on particle position.
Many different systematic studies possible...

Event reconstruction, calibration and alignment concluded.

Detailed performance studies starting, promising first results.

Detailed comparison with dedicated Monte Carlo simulation results about to start...

Full understanding of the test results and validation of the simulation tools can have significant impact on the optimization of the forward calorimeter design...

A dark blue silhouette of a city skyline with various building shapes, including a prominent spire, set against a white background.

Thank you!

Beyond perturbative QED

For $\xi \ll 1$ we are in perturbative regime, lowest order contribution (single photon) dominates, Taylor series in $\alpha \sim \xi^2$ converges fast.

For $\xi \lesssim 1$ - still perturbative regime but slow convergence, onset of multi-photon processes, non-linear effects emerge

For $\xi \gtrsim 1$ - each photon number contribute with comparable weight
 \Rightarrow new approach needed to obtain solutions to “all orders”

Furry picture

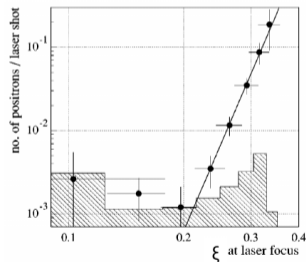
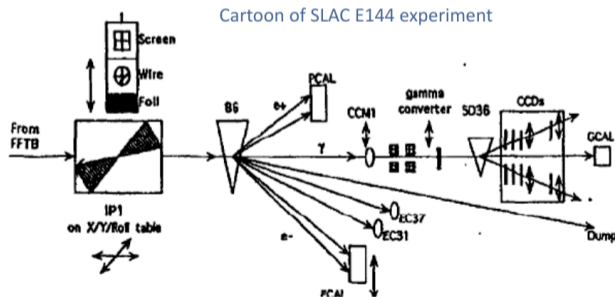
We can factorize electron interactions into “background” interactions with the laser field and actual interactions involving high energy photons ($\omega \gg \omega_L$)

Electrons and positrons “dressed” in laser radiation: Volkov states

SLAC E144

First to approach the non-linear domain was SLAC E144 experiment colliding 46.6 GeV electron beam from SLC with 1 TW green laser ($\xi \lesssim 0.4$ and $\chi \lesssim 0.25$)

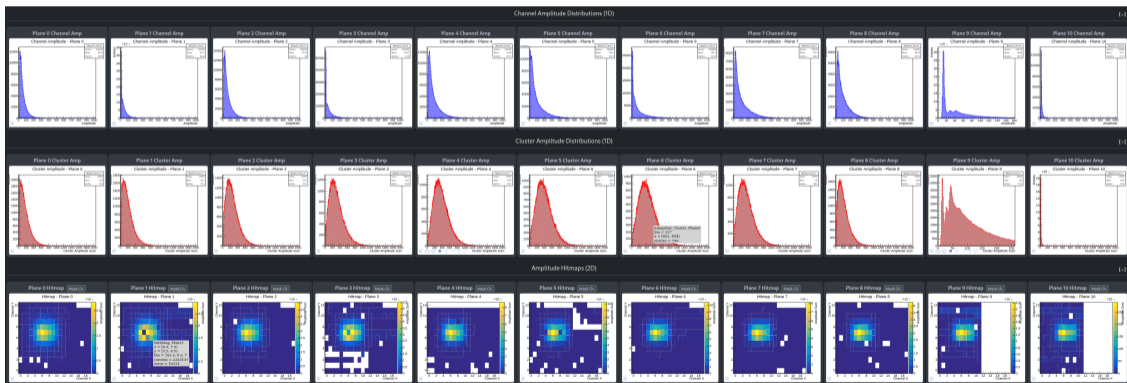
Non-linear Compton scattering and non-linear Breit-Wheeler pair production observed



[Bamber et al. (SLAC 144) '99]

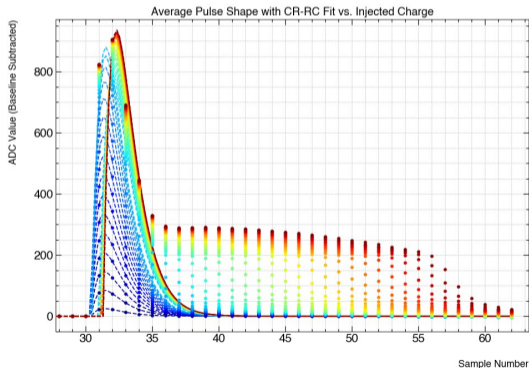
On-line monitoring Zero Suppressed data

Real-time detector monitoring of system performance and data quality via web interface.

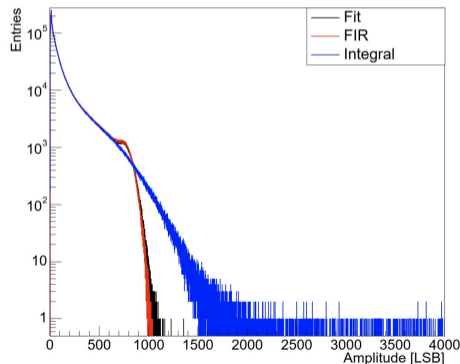


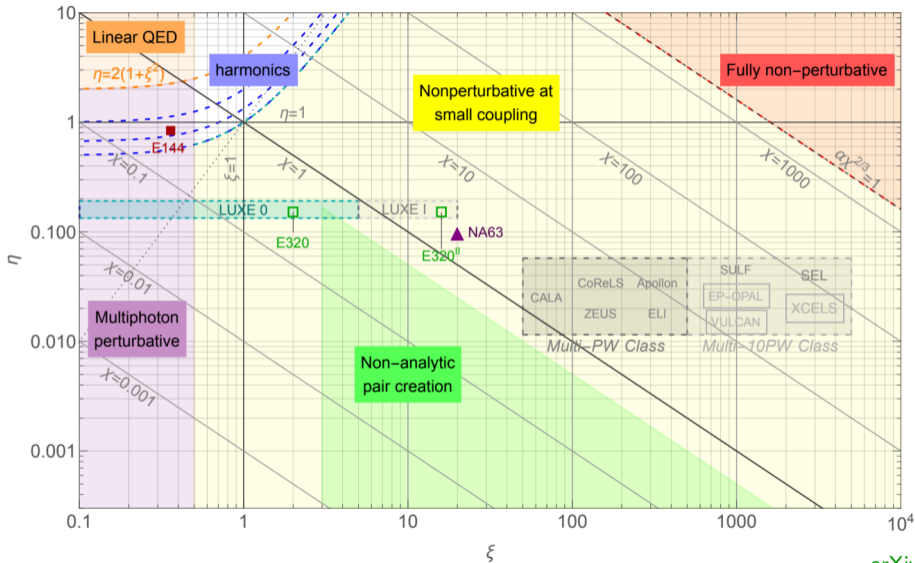
Amplitude correction

FLAME shows linear response up to ~ 200 fC
For higher charges correction is needed...



Example of single channel amplitude spectra
after integral correction (blue)





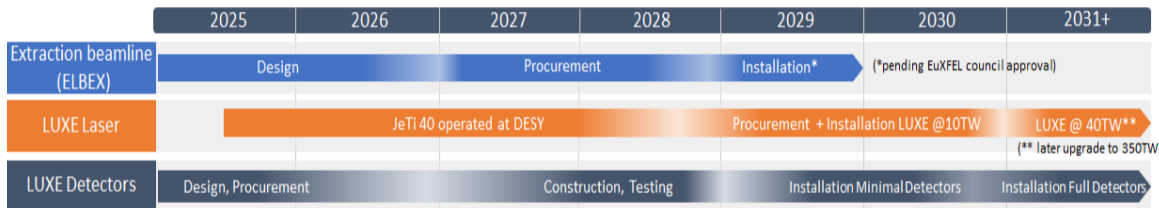
arXiv:2504.00873

Table 3 Laser parameters for the two phases of the LUXE experiment, and the quantum parameter χ_e is given for two different electron energies. All values are for circular polarisation with peak field parameters ξ and χ increasing by a factor of $\sqrt{2}$ for linearly polarised laser irradiation. For focal spot the lowest value targeted is given, and the peak intensity (ξ and χ_e) values given correspond to this waist value. The laser pulse is expected to be Gaussian in all three dimensions in the focal point. The laser is expected to operate at 1 Hz repetition rate, a 10 Hz repetition rate is in principle available at lower intensities

Laser parameters	Phase-0	Phase-1
Fraction of ideal Gaussian intensity in focus (%)	50	
Laser central wavelength (nm)	800	
Laser pulse duration (fs)	25-30	
Laser focal spot waist w_0 (μm)	≥ 3	
Laser repetition rate (Hz)	1-10	
Electron-laser crossing angle (rad)	0.3	
Laser energy after compression (J)	1.2	10
Laser power (TW)	40	350
Peak intensity in focus ($\times 10^{20}$ W/cm ²)	< 1.33	≤ 12
Dimensionless peak intensity, ξ	< 7.9	< 23.6
Quantum parameter	Phase-0	Phase-1
χ_e for $E_e = 14.0$ GeV	< 1.28	< 3.77
χ_e for $E_e = 16.5$ GeV	< 1.50	< 4.45
χ_e for $E_e = 17.5$ GeV	< 1.6	< 4.72

From LUXE TDR: Eur. Phys. J. Spec. Top. 233 (2024) 10, 1709-1974; arXiv:2308.00515

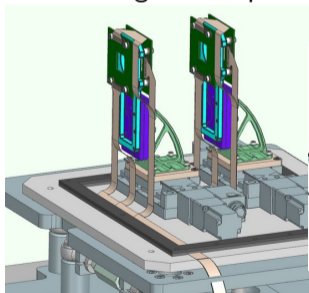
Timeline for the staged construction of the LUXE experiment



[arXiv:2504.00873](https://arxiv.org/abs/2504.00873)

Gamma profiler

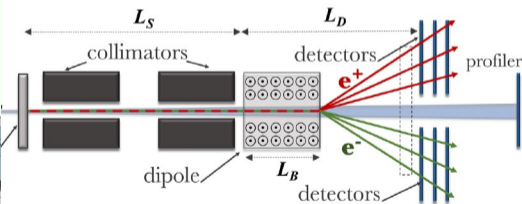
Sapphire micro-strip det.
 $2 \times 2 \text{ cm}^2$, $100 \mu\text{m}$ pitch
 2×2 orthogonal strips



Measurement of beam
width to $< 10 \mu\text{m}$

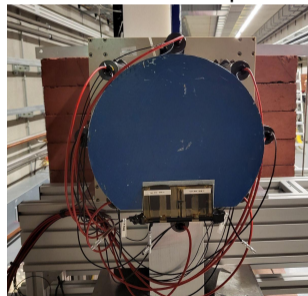
Gamma spectrometer

Photon spectra reconstructed from the
measured Bethe-Heitler e^+e^- pairs
generated in a thin target



Gamma flux monitor

Photon beam position
and intensity from
instrumented dump



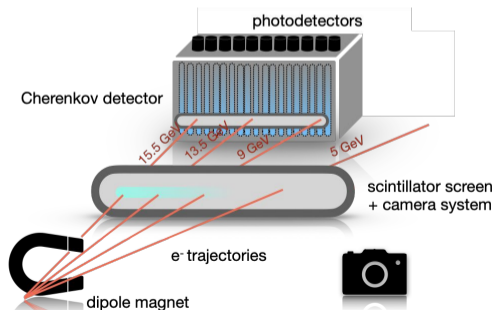
Looking at shower
leakages from the dump

Cherenkov detector

- air-filled steel straws or glass rods
- SiPM readout, 2 mm spatial resolution

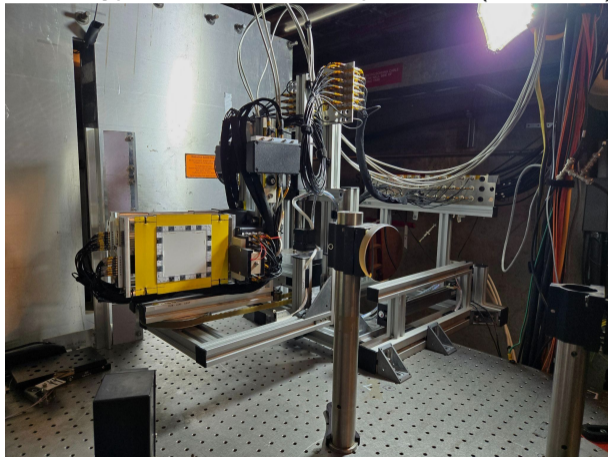
Scintillating screen

- optical readout (camera)
- 0.5 mm position resolution



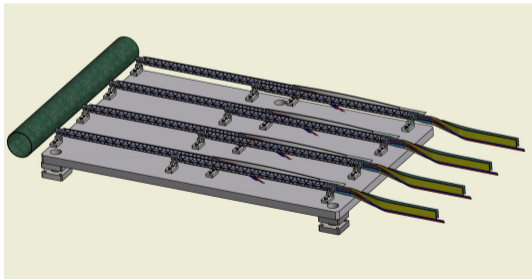
electron detectors for electron-laser mode

Prototype tests at E-320 experiment (FACET-II)

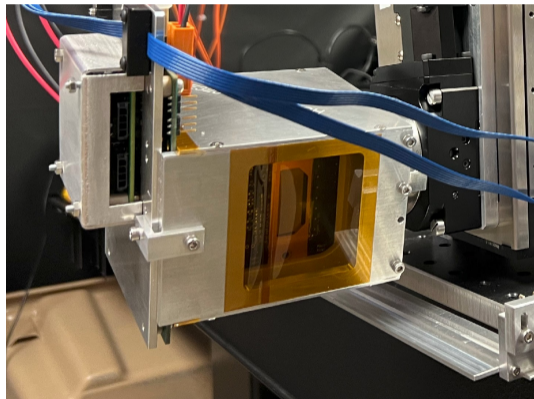


Positron pixel tracker

- Design based on ALPIDE chips (MAPS)
- Four layers, 18 chips per layer in two staves
- Spatial resolution $\sim 5 \mu\text{m}$



Prototype tests at E-320 (FACET-II)

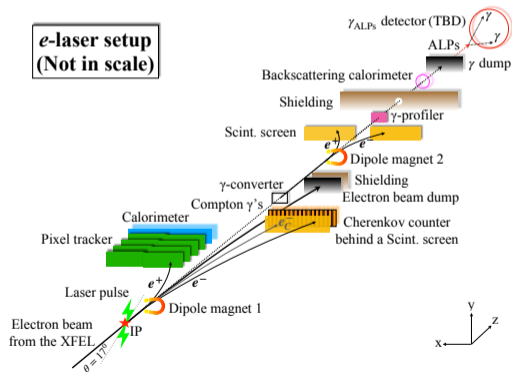


Similar set-up for electron arm in gamma-laser mode

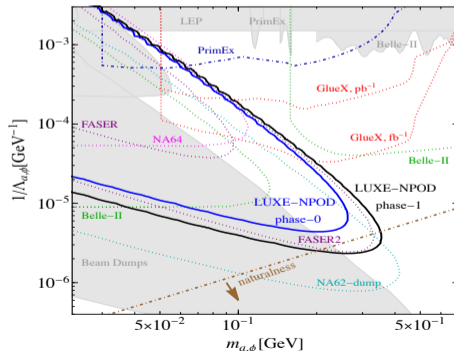
LUXE-NPOD

arXiv:2107.13554

Experimental set-up can be extended to allow for light exotic long-lived particle searches.
 Could be produced directly in electron-laser collisions (“optical dump”) or in photon dump.



Expected reach of axion search



LUXE



membership of Russian institutes suspended